Journal of Engineering and Sustainable Development
Vol. 30, No. 04, July 2026
https://jeasd.uomustansiriyah.edu.iq/index.php/jeasd
ISSN 2520-0917
Research Article
https://doi.org/10.31272/jeasd.3852

Evaluation of Groundwater Development Potential by Using System Dynamics Modeling

Muhammad Ramli[1*], Aryanti Virtanti Anas[1], Asta Arjunoarwan Hatta[1], Hasbi Bakri[2]

[1]Faculty of Engineering, Hasanuddin University, Kampus Unhas Gowa, Indonesia
[2]Faculty of Industrial Engineering, Moslem University of Indonesia, Kampus Makassar, Indonesia

[*]Email: ramli@unhas.ac.id

Article Info

Received	**30/12/2025**
Revised	**06/06/2026**
Accepted	**28/06/2026**

Abstract

Groundwater in aquifers is a very important resource that can flow over long distances to meet the needs of areas that require it. However, its existence beneath the surface requires a good understanding of the water system to manage it properly. This study aimed to develop a system dynamics model to analyze the impact of water balance on the sustainability of groundwater resource development in Parepare, Indonesia. Meeting urban water needs through groundwater use is approximately 4,526,864 m^3/year, significantly larger than surface water at 2,799,948 m^3/year. System dynamics modeling was conducted using STELLA 10.0.4, with a 10-year simulation period. The research results show that this area experiences a rainy season for 9 months and a dry season for 3 months, but groundwater recharge occurs only for 6 months, with recharge potential ranging from 85,858 m^3/month to 62,885,852 m^3/month. Based on the results of the system dynamics modeling, the potential for groundwater recharge remains very high, supporting the development of new groundwater production wells to meet the water shortage, with a capacity of 239,208 m^3/month.

Keywords: Aquifer storage; Groundwater resources; Groundwater wells; System dynamics, Water balance

1. Introduction.

Groundwater is the most important water resource in the world, as it provides almost 99% of the total freshwater [1]. However, one of the biggest problems in the world today is the management of groundwater for sustainable development purposes. Rapid population growth and economic development, especially in the coastal urban areas of developing countries, exacerbate the problem of water resource development. Groundwater experiences significant distribution imbalances and is unsustainably exploited [2]. Recent studies have shown a drastic increase in groundwater extraction in semi-arid basins [3], excessive pumping leading to subsidence [4], and groundwater-level depletion due to overextraction and inadequate replenishment [5]. In Indonesia, many cities rely exclusively on private wells due to inadequate piping systems, thereby increasing urban dependence on groundwater [6]-[8]. The vulnerability of groundwater in tropical coastal areas is further exacerbated by climate change [9], [10].

It is generally agreed that the management, planning, and operation of future water resource systems require modeling. Modeling can assess the impact of specific changes on the surface of an area, including the quantity and quality of water and the condition of the affected groundwater system. Management authorities must ensure the sustainable availability of water while meeting the increasing demand for groundwater. The development of hydrology and water chemistry studies, as well as integrated surface- and groundwater flow models, in a region has been carried out using numerical methods in various areas [11]-[13]. This modeling requires sufficient hydrogeological data to obtain good simulation results. In developing countries, these data are sometimes insufficient to conduct reliable numerical modeling. Consequently, an understanding of groundwater systems is often achieved by developing simple conceptual models [14].

This study aims to address the critical gap in assessing groundwater development potential with limited data. This study innovatively applies system dynamics modeling to integrate water balance, demand forecasting, and sustainability analysis. System dynamics (SD) has evolved into a highly effective method for water resource management because it can explicitly depict stock, flow, and decision feedback. The SD approach has been applied to model groundwater dynamics [15], [16]. SD can be combined with several modeling

approaches, including scenario testing [17], water resource management models for long-term scenario formulation [18], integration of water use across sectors at the groundwater basin scale [3], and hydro-economic SD models for urban groundwater use [19]. SD can be applied to develop conceptual and hydrological models that simulate hydrological and hydrogeological processes and help assess the impacts of economic, social, and political development [20], [21].

The SD modeling in this study was used to evaluate the sustainability potential of groundwater resources in Parepare. The utilization of groundwater in Parepare is quite intensive, with groundwater production of 180.66 L/s, exceeding the surface water utilization of 156.85 L/s [22]. This area is not part of any groundwater basin [23], indicating that the potential groundwater resources have not been adequately identified. Additionally, the area's coastal conditions render groundwater susceptible to seawater intrusion. Therefore, SD modeling emphasizes evaluating the potential development of the groundwater system based on the water balance and the behavior of groundwater management and groundwater users. The analysis was conducted using a conceptual model enhanced with system dynamics to assist in making decisions about groundwater management without highly comprehensive hydrogeological data. The research results provide methodological contributions to validating alternative modeling approaches for regions with limited data.

2. Material and Methods

2.1. Study Area

Parepare city has an area of 99.33 km² and is located at latitude 30^{O}57'39" – 40^{O}04'49" South Latitude and 119^{O}36'24" – 119^{O}43' 40" East. This city has experienced population growth of approximately 2.5%, from 129,542 in 2010 to 160,309 in 2023 [24]-[28]. This is a coastal area bordering the Makassar Strait. Parepare has a flat landscape and undulating hills, with elevations of 0–500 m above sea level, which cover approximately 80% of the hill area. The map of the research location is shown in Fig. 1.

Based on recorded data for 2019-2023 from the Meteorology and Climatology Station [24]-[28], the average temperature is 28.5 °C with a minimum temperature of 25.6 °C and a maximum temperature of 31.5 °C. The city has a tropical climate with two seasons: a dry season from March to September and a rainy season from October to February. February 2023 had the highest rainfall, 1,094.7 mm, and 25 rainy days. The geological conditions of this area and its surroundings are composed of alluvial deposits (Qac), Camba volcanic rocks (Tmcv), Parepare volcanic rocks (Tppv), and marine sedimentary rocks of the Camba Formation (Tmcl), as shown in Fig. 2 [29].

Figure 1. Location of the research area.

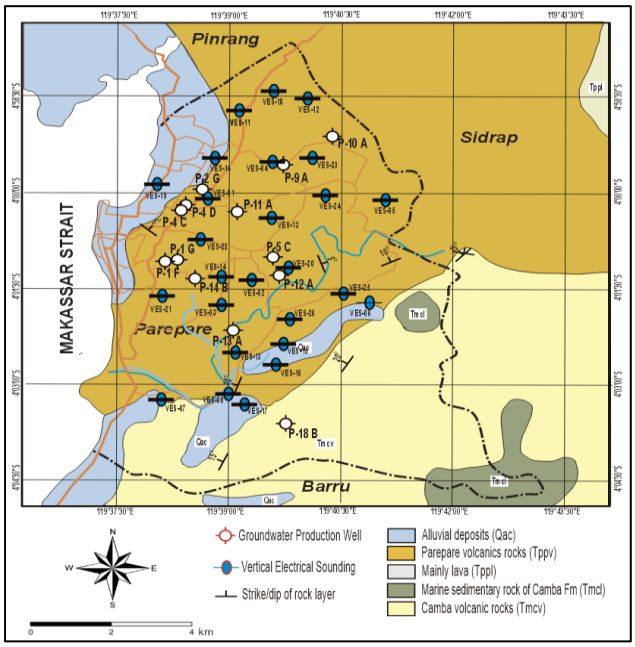

Figure 2. Geological map of the research area [29].

The Alluvial deposits (Qac) consist of clay, silt, mud, sand, and gravel along rivers and coastlines. The Camba Volcanic Rocks (Tmcv) consist of volcanic rocks interbedded with marine sedimentary rock. The rocks that make up this formation consist of volcanic breccia, lava, volcanic conglomerate, and fine-grained tuff to lapilli interspersed with tuff sandstone, calcareous sandstone, mudstone containing plant remains, limestone, and marl. The Parepare Volcanic Rocks (Tppv) consist of tufa, fine-grained to lapilli breccia, and volcanic conglomerate, with inserts of lava sandstone and tuff found in several places. Some volcanic rocks in the eastern region primarily consist of lava (Tppl) with a trachyte structure and contain a large amount of biotite. The Camba Formation (Tmcl) consists of marine sedimentary rocks interspersed with volcanic rocks. These rocks consist of tuff sandstone interspersed with

tuff, sandstone, siltstone, mudstone, marl, conglomerate limestone, volcanic breccia, and coal. In addition, there are limestone members of the Camba Formation (Tmcl), which consist of limestone, tuffaceous limestone, and sandy limestone with tuff inserts.

2.2. Water Balance Calculation

In an aquifer basin, the water balance significantly affects groundwater availability. Water balance includes several processes: precipitation, surface runoff, evapotranspiration, and infiltration. Groundwater originates from rainwater, which infiltrates and percolates into the ground. Infiltration occurs through the unsaturated zone to the groundwater surface, often referred to as groundwater recharge. Therefore, in this study, a surface water balance analysis was conducted to predict the amount of water recharging into the aquifer. The mathematical relationship of the hydrological cycle as a water balance is expressed by (1) [30], [31].

$$P = AET + R + GR \pm \Delta S \quad (1)$$

where P is precipitation (L/T), AET is the actual evapotranspiration (L/T), R is runoff (L/T), GR is groundwater recharge (L/T), and ±ΔS is the variation in groundwater storage (L/T). The last two parameters, GR and DS, are expressed as groundwater potential.

Water balance analysis was performed using rainfall and climate data from the Central Statistics Agency, covering the period 2019–2023. The data were accumulated or averaged monthly. The calculation of evaporation potential in this study uses the Penman Method, as formulated in (2) below. Equation (2) considers climate parameters, including temperature, wind speed, air humidity, and sunshine duration [32].

$$ETo = c\big(W \times Rn + (1 - W) \times f(U) \times (ea - ed)\big) \quad (2)$$

Where ETo is the monthly evapotranspiration (mm/day), c is a correction factor due to climate conditions, W is the weight factor, Rn is the net radiation (mm/day), ea is the saturated vapor pressure (mbar), ed is the actual vapor pressure (mbar), and f(U) is the wind speed function. This equation estimates evapotranspiration by combining energy and aerodynamic factors, with each component playing an important role. The radiation component (W × Rn) describes the energy available for water evaporation. The aerodynamic component ((1-W) × f(U) × (ea-ed)) describes the ability of the atmosphere (wind and humidity) to transport water vapor. Constant c is an adjustment of the calculation results to fit local conditions.

Another parameter of the water balance is surface runoff. Surface runoff was calculated using a dimensionless runoff coefficient to convert rainfall into runoff. This coefficient represents the integrated effects of catchment loss, including soil surface properties, slope, saturation level, and rainfall intensity. The surface runoff coefficient values used in this study were obtained from Goel [32] and are listed in Table 1.

2.3. System Dynamics Modeling

System dynamics modeling is a computer simulation procedure developed to understand the performance of complex systems over time and to design alternative solutions that improve the ability to extrapolate and interpolate in a broader context meaningfully. Interdependent variables, mutual interactions, information feedback, and circular causality characterize system dynamics. This modeling approach originates from management and engineering but has been developed as a valuable tool for analyzing social, ecological, economic, physical, chemical, and biological systems. It has also been used to integrate complex hydrological data with other information (e.g., policies, regulations, and management criteria) to produce a decision-support system.

Table 1. Coefficient of runoff based on land use [32]

Type of area	Runoff coefficient
Urban	0.30 – 0.50
Forest	0.05 – 0.20
Commercial and industrial	0.70 – 0.90
Parks and pastures	0.05 – 0.30
Pavement and roads	0.70 – 0.95
Flat agriculture	0.10 – 0.50
Highly agriculture	0.30 – 0.70

The software used for modeling the system dynamics of the water balance was STELLA 10.0.4. The main steps in developing a system dynamics simulation model are as follows.

(1) Problem articulation: This modeling was performed to simulate the availability of rainwater as a source of recharge into the aquifer. Therefore, the simulation was based on a water balance system that accounted for conditions over the last five years, namely 2019-2023. Simulations were performed to predict the conditions until 2028.

(2) Dynamic hypothesis formulation. In this stage, an initial hypothesis is formulated by dividing the system into sectors, with each sector depicted as a causal loop diagram that defines critical variables. In general, groundwater demand will increase with city development, while recharge decreases due to changes in land cover. All water balance parameters will be analyzed comprehensively to study future conditions in groundwater management.

(3) Formulation of simulation models. This stage prepares the model structure by transforming the sector causal loop diagram into a system dynamics model that includes data and mathematical relationships among the variables. The simulation model was prepared by predicting rainfall events, evapotranspiration, and recharge changes for each land-cover type, including calculating the increase in water demand based on development trends over the last five years.

(4) Policy design and evaluation. At this stage, system dynamics models are used to understand system behavior and implement management policies and scenarios. The scenarios in this study were developed from the model's

primary key variables that had the greatest impact on the groundwater balance. The effect was determined by analyzing the model's sensitivity to changes in parameter values.

In general, the research method is illustrated using a research flowchart, as shown in Fig. 3. The research focuses on a simple conceptual aquifer model that considers the potential of recharge as a groundwater source relative to increasing water demand due to urban development. Furthermore, to meet this demand, the potential of surface water is considered more challenging for increasing production capacity owing to landscape and surface water conditions. Therefore, the potential to meet water supply shortages is focused on analyzing groundwater potential.

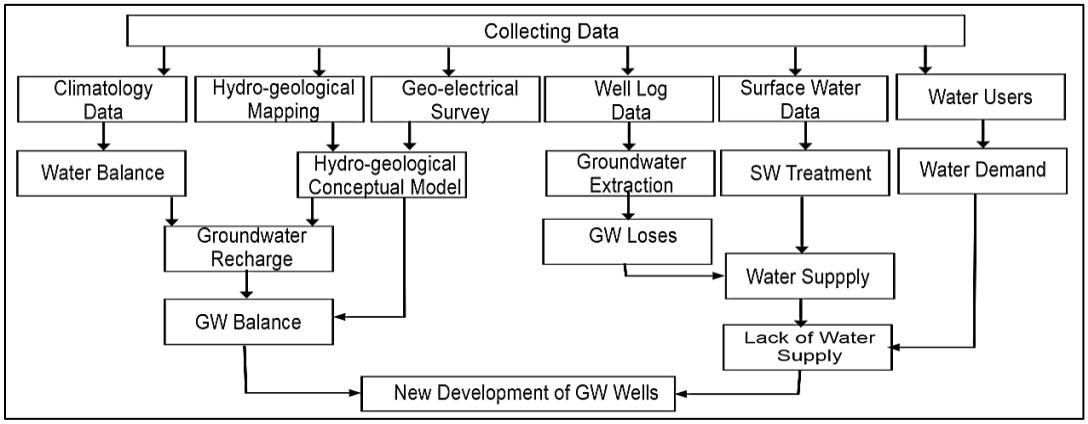

Figure 3. Flow chart of research methodology

The flowchart is a systematic, data-driven approach in which research activities begin with the collection of climatological, surface hydrogeological, geoelectric, well-log, surface-water, and water-user data. These data were analyzed to calculate the water balance, develop a conceptual hydrogeological model, and assess groundwater production and water loss, surface water treatment capacity, and water demand. The results of these analyses were then integrated into the groundwater balance, which is the relationship between groundwater recharge, water balance, and the conceptual hydrogeological model. On the other hand, the lack of water supply was estimated as the difference between demand and available water supply. All data and analyses were used to evaluate the potential development of new groundwater production wells.

3. Conceptual Model of the Groundwater Balance

3.1. Hydrogeological Setting

The hydrogeological system of Parepare City is structured with consideration of the water components entering and leaving the aquifer. This hydrogeological system depends on morphology, lithology and stratigraphy, and geological structure, which influence the aquifer system and groundwater movement beneath the surface. Analysis of groundwater balance requires a good understanding of the interactions between surface water and groundwater in a conceptual model (Fig. 4). The data used to develop this conceptual model were geological data [29], geoelectric (vertical electrical sounding/VES) data, groundwater drilling data [22], water utilization [20], and city statistical data in documents of municipalities in figures [24]-[28]. The available statistical data include rainfall, meteorology, agricultural activities, and industrial development.

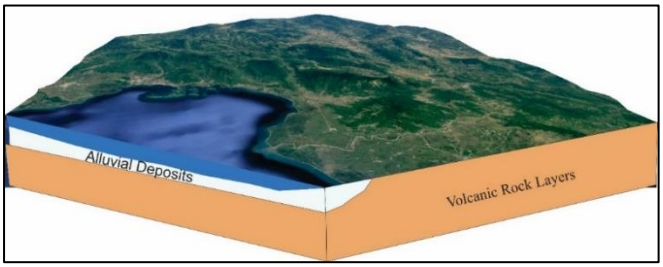

Figure 4. Conceptual model of the groundwater system.

As mentioned above, the geological conditions indicate that this area generally consists of volcanic rocks interspersed with marine sedimentary rocks. Based on the interpretation of the geoelectric survey data and groundwater production well drilling data listed in Table 2, the aquifer layers can be divided into unconfined and confined aquifers. Groundwater is divided into shallow (phreatic) and deep groundwater based on depth. The unconfined aquifer is located 15-40 meters below the surface, whereas the confined aquifer is found at depths between 40 and 100 m. At greater depths, there is a bedrock layer composed of lava with resistivity values in the tens of thousands of ohm-m. In coastal areas, the aquifer layer is infiltrated by seawater, as indicated by shallow resistivity values in the rock layer.

Table 2. List of groundwater production wells.

No.	Well Code	X Latitude	Y Latitude	Well's Capacity (liter/sec)
1	P-1 F Harapan	119°37'59.5"E	4°01'04.5"S	20
2	P-1 G Harapan	119°38'03.7"E	4°01'04.9"S	5
3	P-2 G Soreang	119°38'18.5"E	3°59'54.5"S	30
4	P-4 C Takkalao	119°38'08.0"E	4°00'16.2"S	10
5	P-4 D Takkalao	119°38'08.0"E	4°00'16.3"S	20
6	P-5 C Wekke'e	119°39'16.6"E	4°01'01.9"S	20
7	P-14 A B_Runcing	119°38'19.0"E	4°01'20.9"S	12
8	P-8 B Ladoma	119°39'22.1"E	4°03'32.0"S	20
9	P-9 A Lapadde	119°39'24.8"E	3°59'41.4"S	10
10	P-10 A Lanyer	119°40'02.4"E	3°59'10.0"S	10
11	P-11 A Tegal.	119°38'51.0"E	4°00'18.3"S	20
12	P-12 A G_Obat	119°39'20.6"E	4°01'16.1"S	20
13	P-13 A G_Mandiri	119°38'46.8"E	4°02'8.45"S	10

The city of Parepare is part of an aquifer basin covering approximately 600 km². Pratikno estimated the availability of groundwater in this basin to be 1.34 million m³/year in the unconfined aquifer and 5.00 million m³/year in the confined aquifer [33]. The availability of groundwater is considered as the potential groundwater from subsurface flow, which can be estimated at 528,750 m³/month.

Land use patterns largely determine the availability of groundwater in aquifers. The main problem in urban areas is the low infiltration of rainwater into the ground. In this area, several rain catchment areas are becoming critical [34]. This will, of course, impact on the overall groundwater availability. The increase in population and the need for residential and office land will further reduce groundwater recharge rates. In contrast, the increase in water demand will continue, which is a relationship that needs to be considered in city management.

3.2. Water Balance and Groundwater Storage

The groundwater system is closely related to the hydrological cycle, which includes several processes: precipitation, surface runoff, evapotranspiration, and infiltration. Groundwater originates from rainwater that infiltrates and percolates into the ground. Infiltration occurs through the unsaturated zone to the groundwater surface, often referred to as groundwater recharge. Evapotranspiration is the loss of water from plant tissues and soil surfaces. Potential evapotranspiration was calculated based on climatological data. Some rainwater that falls onto the land surface flows to rivers, lakes, or oceans and is called surface water runoff. The relationship between these parameters is expressed by the water balance equation, as shown in (1).

The research area is in a tropical rainforest climate in the southern hemisphere. The southern hemisphere experiences the rainy season from November to March. During this time, the tropical northern hemisphere experiences a dry season with reduced rainfall, and the days are usually sunny. From May to September, the rain belt shifts northward, and the southern tropical region experiences a dry season [35]. Rainfall data recordings for the years 2019-2023 in the research area varied from 0.00 to 1,094.70 mm/month. The average monthly rainfall over five years ranged from 37.26 mm/month in July to 702.08 mm/month in January. In the Köppen climate classification, a dry season month in tropical climates is defined as a month with average precipitation below 60.00 mm. Therefore, in this area, the dry season occurs from July to September and the rainy season from October to June. The distribution of the average monthly rainfall is illustrated in Fig. 5.

The next parameter is evapotranspiration, which is the loss of water from the soil either through evaporation from the soil surface or transpiration from the leaves of the plants growing above it. Evapotranspiration is an important parameter in water balance calculations because it significantly contributes to water loss from soil during plant growth. The rate of evapotranspiration is influenced by the amount of solar radiation, atmospheric vapor pressure, temperature, wind, and soil moisture, which in this case is calculated using the Penman Method, as explained in (2) above. Several climatological parameters are related to temperature, humidity, wind speed, and sunlight duration. The results of the monthly evaporation calculations over the past five years are shown in Fig. 6.

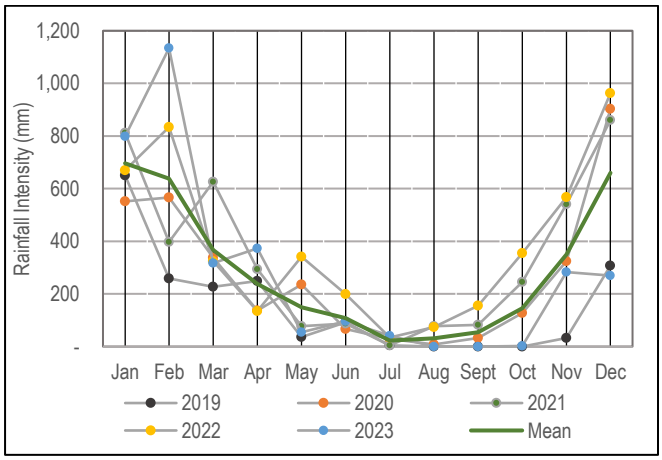

Figure 5. Average monthly rainfall in 2019-2023.

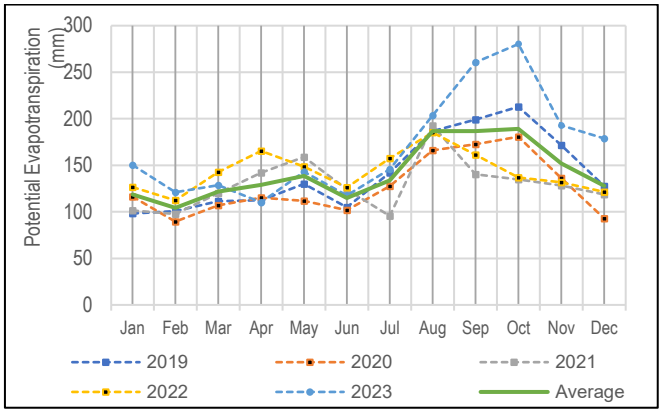

Figure 6. Monthly potential evapotranspiration in 2019-2023.

In the graph, potential evapotranspiration values range from 89.52 mm/month in February 2019 to 280.30 mm/month in October 2023, with an average of 141.94 mm/month. Generally, from January to August each year, conditions over the last 5 years have been relatively uniform, whereas from September to December, evapotranspiration values fluctuate more.

The water balance system is also related to surface runoff. Estimating surface runoff involves calculating the amount of water from precipitation that flows over the land surface and eventually reaches the rivers, streams, and lakes. The proportion of rainfall that becomes surface runoff can vary significantly; this proportion is known as the surface runoff coefficient. This is influenced by the amount of rainfall, watershed characteristics (such as size, slope, soil type, and vegetation), and land-use patterns. In this study, the runoff coefficient was calculated using a land-use pattern approach. As cities develop, changes in land use become the most sensitive issue.

Data from the Central Statistics Agency divide land use into nine criteria: rice fields, unused land, community forests, state forests, settlements, fishponds, moorlands, grasslands, and yards, with the distribution in 2020 shown in Fig. 7 and Table 3. In the 2019-2023 period, there was a decrease in two types of land use, namely vacant land and grassland, while an increase in the land area occurred in pond fish [24]-[28]. The magnitude of the changes for the four types of land use was approximately 0.01 km2, which, in this case, was considered insignificant. Therefore, the calculation of surface runoff values assumes that the type and extent of land use will remain constant until 2028.

The surface runoff coefficient was calculated using the coefficient value approach published by Goel, as shown in Table 1. Because the research area is a hilly region and meets the criteria for an intermediate city, the coefficient used is the highest. The area of each type of land use was weighted against the city's total area. The calculation results showed that the surface runoff coefficient was 0.254 of the rainfall. The detailed calculations are presented in Table 4.

Rainwater that falls to the earth's surface undergoes evapotranspiration and infiltration, and the remaining water flows as surface runoff. Rainwater that infiltrates the ground becomes groundwater. Water availability is the amount of water in an area through the hydrological cycle, including surface water, groundwater, and rainfall. Water moves in a balanced cycle on land surfaces and in soil. Groundwater recharge is a general term for infiltration. The water balance approach is one of the techniques used to evaluate groundwater recharge. In this case, changes in infiltration and storage are assumed to be GR parameters in (3), which can be considered groundwater stores.

$$GR = P - AET - RO \quad (3)$$

Where GR is aquifer recharge from precipitation, P is precipitation, AET is actual evapotranspiration, and RO is runoff. Fig. 8 shows the estimated groundwater recharge from the water balance calculation, where part of the rainwater that falls on the ground surface becomes surface runoff or is lost to evapotranspiration, and the remainder recharges the soil.

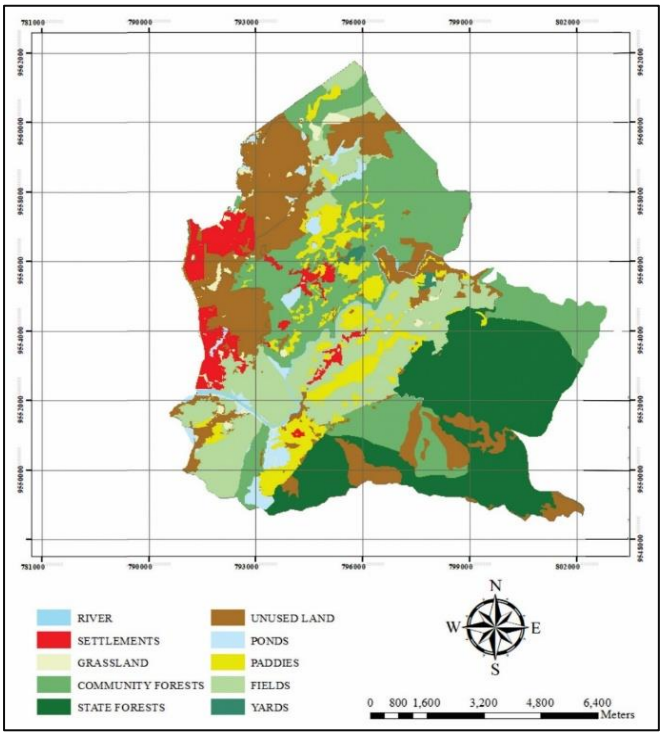

Figure 7. Land use map of Parepare in 2020.

Table 3. Development of land use of Parepare Area (km^2).

Land Use Type	2020	2021	2022	2023	2024	Average
Paddies	7.63	7.63	7.63	7.63	7.63	7.63
Unused land	21.24	21.24	21.23	21.23	21.23	21.24
C. forest	24.46	24.46	24.46	24.46	24.46	24.46
State forest	21.38	21.38	21.38	21.38	21.38	21.38
Settlement	4.24	4.24	4.24	4.24	4.24	4.24
Fishpond	2.48	2.49	2.49	2.50	2.50	2.49
Field/moor	16.17	16.17	16.17	16.17	16.17	6.17
Grassland	1.38	1.38	1.37	1.37	1.37	1.37
Yard	0.35	0.35	0.35	0.35	0.35	0.35
Total area						89.33

Table 4. Estimation of runoff coefficient of the research area

Land Use Type	Area size	Equivalence to Goel's criteria	Runoff Coeff	
			Max	Proportional
Paddies	7.63	Hilly agriculture	0.700	0.053
Unused land	21.24	Hilly agriculture	0.700	0.149
Community forest	24.46	Forest	0.200	0.049
State forest	21.38	Forest	0.200	0.043
Settlement	4.24	Commercial and industrial	0.900	0.038
Fishpond	2.49	Flat agriculture	0.500	0.012
Field/moor	6.17	Parks and pastures	0.300	0.019
Grassland	1.37	Parks and pastures	0.300	0.004
Yard	0.35	Hilly agriculture	0.700	0.002
Total area	89.33			0.369

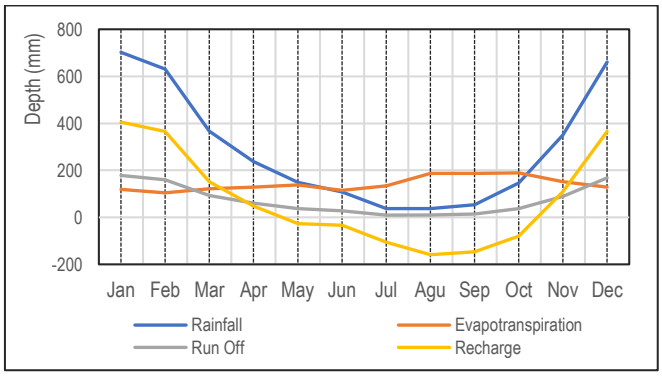

Figure 8. Average monthly water balance.

3.3. Water User Population

In many places, water needs are met with surface water; however, this cannot be done in Parepare City due to landscape conditions and the location of surface water sources. The City Government uses more groundwater than surface water. A large-scale groundwater development project was conducted in 2016-2017, and new development requires significant investment. Thus, the sustainability of the groundwater supply in the area was analyzed under current conditions. Water resource management should be improved and closely linked to specific community development goals [36]. Approaches must consider the unique needs and challenges of local communities and ensure that water resources are managed sustainably and fairly. This study analyzed groundwater needs based on population, livestock type, and industry. The development of these three variables in Parepare from 2019 to 2023 is presented in Table 5.

Table 5. Data for Population (people), Livestock (heads), and Industry (companies) in Parepare City.

Year	Population (person)	Livestock (animal unit)			Industries (units)
		I	II	III	
2019	148,265	5,457	3,923	1,334,976	1,348
2020	150,987	5,077	3,218	977,794	1,372
2021	152,922	4,812	2,484	818,344	1,243
2022	154,854	5,431	2,994	811,027	1,149
2023	160,309	6,050	3,504	804,904	1,055

The estimation of the water needs of each type of water user is based on the Indonesian National Standard SNI-6728.1:2015, issued in 2015, concerning the Preparation of Spatial Accounts for Natural Resources-Water Resources Section [37]. The amount of water required is estimated based on the population and the standard needs of the area's residents. Calculations of industrial water requirements are generally constant over time. The number of workers, the area of industrial waters, and the type of industry were considered when calculating industrial needs. Another water requirement is for livestock, depending on the livestock population and type.

4. Results and Discussions

4.1. Analysis of Groundwater Balance and Water Demand

The integration of water balance parameters into the hydrogeological conceptual model in system dynamics modeling is presented as a causal loop diagram. A causal loop diagram shows the relationships among these variables and the feedback processes (Fig. 9). It is useful for understanding the system structure and the origins of system behavior patterns. When a system element indirectly affects itself after a delay, the part of the system that is affected is called a feedback loop. Every decision is made in a feedback loop, a closed loop between cause and effect. In a loop, the response of each element, based on whether it has an upward or downward impact on the variable, is marked with a (+) or (-) sign. Furthermore, a causal loop diagram was structured as a stock-and-flow model to describe the groundwater balance system in detail.

The causal loop diagram shows that most variables are positively related, meaning that an increase in one variable will encourage increases in the other connected variables. Rainfall increases surface runoff, which can enhance groundwater recharge, thereby improving the groundwater balance. The number of wells and their capacity increased groundwater extraction but also contributed to groundwater losses, which reduced groundwater storage. This causal loop illustrates that the groundwater balance is a complex interaction between natural factors (rainfall, evapotranspiration, and runoff) and socioeconomic factors (population, industry, livestock, and number of wells). The groundwater availability loop, with parameters including rainfall, runoff, recharge, evapotranspiration, and groundwater storage, and the total water demand loop, which depends on the growth of population, industry, and livestock, are factors that influence the development potential loop and the groundwater development demand loop, which are the determining variables for the groundwater balance.

The dynamic groundwater balance model was designed to evaluate the potential development of groundwater production wells to meet water demand until 2028. The stock-and-flow diagram in Fig. 10 illustrates the relationships among the parameters involved. The stock-and-flow diagram accounts for the time dependence of relationships among variables and includes formulas and constants to support the simulation. Several factors to consider are water balance, groundwater production, surface water supply, and water demand predictions.

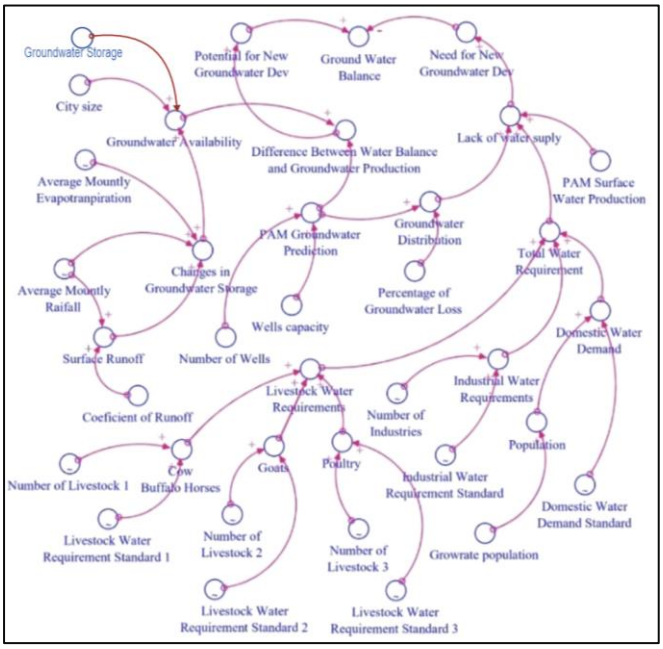

Figure 9. Causal loop diagram of groundwater balance.

In the stock-and-flow diagram in Fig. 10, the potential for groundwater well development is represented by a groundwater balance. This value represents the accumulation of recharge potential and groundwater production. The recharge potential is the difference between rainfall and the sum of evapotranspiration and surface runoff. Next, the calculation of well development needs is based on the predicted water demand, driven by growth in the water-user population (residents, livestock, and industry), minus the water availability from groundwater wells and surface water sources.

This stock-and-flow diagram shows that groundwater is the main stock, influenced by hydrological flows and water needs, with various feedback mechanisms determining whether the system remains balanced or experiences a water crisis. The main stocks are groundwater storage and water demand. Groundwater storage, which consists of groundwater stored in aquifers, is the primary stock. Its value changes according to the rates of recharge, evapotranspiration, runoff, and changes in groundwater storage (in addition). The water demand stock is all water needs that will accumulate in the total water requirement, which depends on population growth, increases in the number of industries, and growth in livestock (cows, buffalo, horses, poultry). Therefore, the groundwater balance is determined by the interaction between hydrological inputs (rainfall, runoff, and recharge) and demand outputs (domestic, industrial, and livestock).

SD modeling uses a water balance based on the average of the last five years of events, as previously explained. This was intended to calculate groundwater availability, which is the difference between monthly rainfall, evapotranspiration, and surface runoff. The depth of the difference was multiplied by the area of Parepare to determine the volume of groundwater storage in the aquifer. This monthly condition was assumed to be constant throughout the simulation period. The estimation of groundwater presence also considered an underflow of

528,750 m³/month. In calculating water needs for population growth, a growth rate of 2.5% was used, based on data from 2010-2023, with an initial population of 148,265 residents. The development of livestock and industry was predicted at random for 2019-2023. Furthermore, the production of bore wells and surface water was assumed to remain constant during the simulation, using average monthly production.

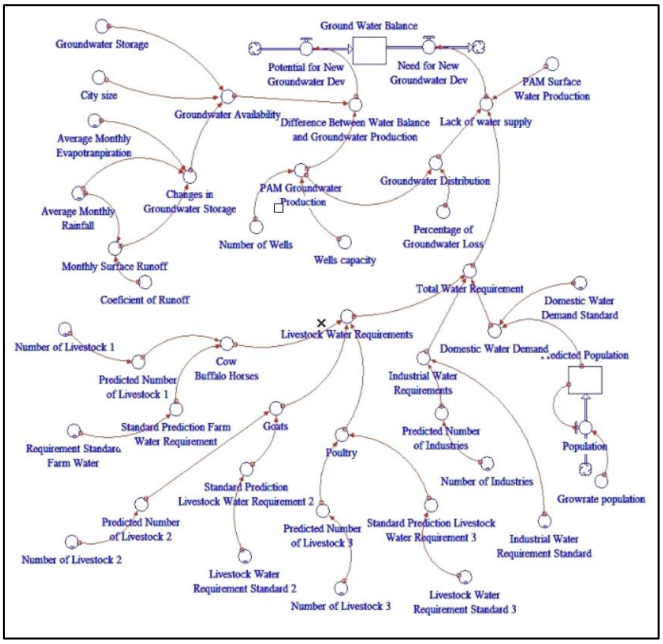

Figure 10. Stock-and-flow diagram of groundwater balance.

The sub-model influenced this SD for predicting urban water demand, as shown in Fig. 11. To meet current water demand, the government has implemented a policy to utilize surface water and groundwater managed by the Regional Drinking Water Company. Groundwater is considered more efficient for distribution than surface water due to the area's hilly terrain. Therefore, in 2022, large-scale groundwater development was carried out, resulting in much higher groundwater production than surface water, as shown in Table 6.

Table 6. Monthly water production and groundwater production losses in 2022.

Months	Surface Water (m³/month)	Groundwater (m³/month)	GW production loss (%)
January	241,350	396,095	48.25
February	221,647	340,669	42.92
March	238,878	361,341	49.09
April	243,784	367,026	45.06
May	251,742	391,957	47.04
June	233,825	373,866	47.45
July	235,269	394,753	51.00
August	247,999	395,218	46.94
September	234,523	366,027	45.54
October	248,715	361,068	45.52
November	181,610	384,630	47.85
December	220,606	394,214	49.97

Based on these considerations, the water requirements of Parepare City were calculated. This city is experiencing approximately 8% population growth, with a population of 160,000 in 2023. Therefore, it is classified as a medium-sized city with water needs between 100 and 125 liters/day/person (in this case, 110 L/day/person is used). Other calculations of water requirements include Group I of livestock consisting of cows, buffalo, and horses with a water requirement of 40 L/day for one animal, Group II goats and sheep of 5 L/day, and Group III poultry with a water requirement of 0.60 L/day. Finally, industrial water demand was calculated based on the number of workers, the area served by industrial water, and the type of industry, and was estimated at 1,200 L/day/industry. The prediction of water demand for the three types of water users is based on population growth projections and predictions with a random function for livestock and industrial needs. The predicted total water demand for 2019-2028 is shown in Fig. 11.

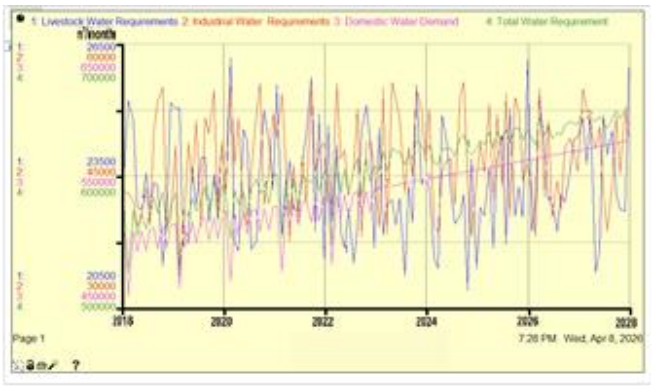

Figure 11. Changes in total water demand in relation to the growth of water users 2019-2028 (m³).

Fig. 11 shows the development of water demand from 2018 to 2028, with a consistent upward trend across all water-user sectors, including domestic, industrial, and agricultural. Domestic needs, represented by the pink line, show a relatively stable year-over-year increase, with an average of 535,246 m3/month, ranging from 457,158 m³/month to 576,249 m³/month. The industrial demand, shown by the red line, and livestock demand, presented by the blue line, are relatively stable. The industry's water demand fluctuates between 34,713 and 55,680 m3/month, with an average of 46,617 m3/month, whereas for livestock farming, it fluctuates between 20,856 and 26,187 m3/month, with an average of 20,856 m³/month. Thus, the total water demand indicated by the green line is the accumulation of the three variables. The pattern is smoother because it is a combination, but it clearly shows an increasing trend from approximately 522,976 m³/month in 2018 to nearly 651,575 m³/month in 2028. This increase indicates greater pressure on water resources, making sustainable management crucial.

Water governance in this region faces two main issues: a water supply that does not meet demand and a high percentage of groundwater production loss due to the quality of the water distribution network. Data from 2022 showed that the percentage of groundwater production loss ranged from 42.92%

to 51.00%. Furthermore, the analysis of the relationship between water availability and demand indicates that from 2025 to 2028, there will be a supply shortage of 196,905 to 239,208 m^3/month.

Figure 12 shows the trend of increasing water scarcity, with a pattern similar to that of water demand. This is due to an estimate of increased water demand based on growth in population, livestock, and industry, while the water supply is assumed to remain constant over 10 years. Changes in well conditions may bias this, but in this writing, data on changes in well capacity since its development in 2017 are not yet available.

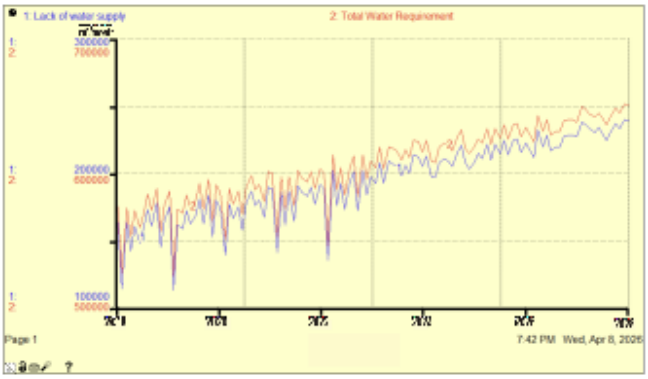

Figure 12. Prediction of water supply shortages against demand by utilizing the current production scheme.

4.2. Potential for New Groundwater Development

In the explanation above, it was stated that one of the causes of unmet water supply is the high percentage of groundwater production loss, which reaches 47.22% per month. This value exceeds the allowable water loss threshold based on the Water Management Regulation of the Ministry of Public Works and Public Housing No. 27/PRT/M/2016 concerning the Implementation of Drinking Water Supply Systems [38], which stipulates that the handling of water loss can be considered achieved if the maximum water loss percentage is 20. The main causes of water loss in the regional drinking water company's pipe network are pipe leaks, overflow from storage tanks, unauthorized consumption, inaccuracies in customer meters, and data-handling errors. Among these causes, the water management authorities recognize that the distribution network is the main contributor due to the area's hilly terrain. Therefore, the development of new groundwater production wells is a policy that must be considered.

This SD model simulates the impact of changes in the water balance on groundwater availability as part of efforts to develop groundwater in the research area sustainably. Given that efforts to increase the water supply focus on utilizing groundwater, this analysis examines the potential to develop new groundwater sources. Thus, surface water utilization was assumed to be constant during the simulation period. Groundwater in the aquifer is extracted by 13 production wells, with a combined capacity of 377,239 m³/month. The groundwater supply is supplemented by the use of approximately 213,237 m3/month of surface water to meet urban water needs. This groundwater facility was created as part of a development project in 2017. The evaluation of this condition shows that since 2019, there has been a supply shortage of approximately 111,515 m3/month, which is expected to increase to nearly 239,208 m^3/month if no new sources are developed.

Fig. 13 shows the relationship among the need for developing new groundwater sources, development potential, and groundwater balance. The development potential is primarily based on the potential excess monthly rainfall that can recharge groundwater. In this prediction, rainfall, evapotranspiration, and surface runoff events were used, with averages of monthly occurrences based on data from 2019-2023. This condition is assumed to have a cycle with the same monthly variation each year; thus, the pattern graph and the added values repeat the same pattern each year. Climatological records indicate that the rainy season lasts 9 months, from October to June, and the dry season lasts 3 months, from July to September. However, model predictions show that replenishment potential occurs only for six months each year, from November to April.

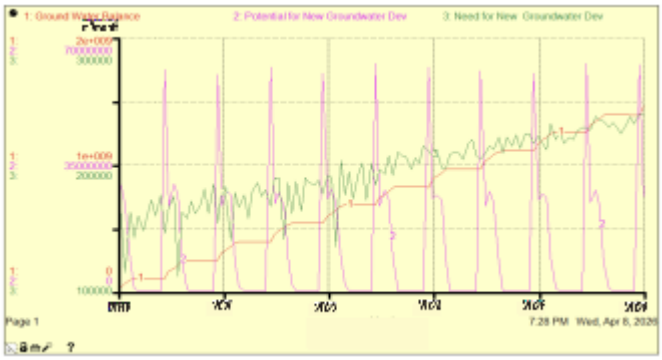

Figure 13. Simulated groundwater balance for 2019-2028.

The graph in Fig. 13 shows that potential groundwater development fluctuates significantly, occurring only 6 months each year, and ranges from 84,858 m3/month to 62,885,852 m^3/month. The average development potential is approximately 12.59 million m^3/month. The potential recharge value may initially seem very high because it considers only the surplus from evapotranspiration and surface runoff, neglecting the aquifer's capacity to store it. An evaluation of the aquifer's storage capacity requires more intensive subsequent studies. However, field conditions show the emergence of several artesian wells that flow year-round, indicating significant groundwater potential. Next, the need for new well development also shows an upward trend, with values ranging from 111,515 m³/month to 239,209 m³/month. Based on the conceptual hydrogeological model, the subsurface flow entering or exiting the aquifer was estimated to be 528,750 m³/month [33]. However, the simulation results in Fig. 13 indicate that groundwater storage accumulation can increase by up to 1.45 billion m³ by 2028.

The results of the analysis above indicate that sustainable groundwater development can still be achieved. The main consideration is that the potential for new groundwater development of 12 million m³/month is still far greater than the need for new well development, which averages 193 thousand

m³/month. This indicates that the groundwater potential still supports further development to meet groundwater demand. This condition indicates significant value; however, more specific studies are needed to evaluate the aquifer's capacity to store groundwater.

5. Conclusions

This groundwater development area consists of volcanic rock deposits with distinctive characteristics, making it somewhat difficult to reconstruct the aquifer layers beneath the surface. Therefore, groundwater potential was analyzed using system dynamics modeling, including water balance, water demand prediction, and sustainable groundwater management, based on a conceptual aquifer model. Monthly rainfall data showed that the rainy season lasted 9 months, but simulations indicated that aquifer recharge could occur only for 6 months per year. Without considering the aquifer's storage capacity, the groundwater potential can reach up to 150 million m³ per year, far exceeding the need for new groundwater development to meet water demands until 2028, which is approximately 239 thousand m³/month. The presence of several artesian groundwater production wells around the contact between the volcanic aquifer and the alluvial deposits also indicates the high potential of groundwater.

Acknowledgements

The authors would like to thank the Institute for Research and Community Service at Hasanuddin University for their financial support for this research under the Unhas 2022 Collaborative Basic Research Scheme. We would also like to express our deep gratitude to the Regional Water Company of Parepare City for facilitating the acquisition of data on groundwater production wells and the customer service systems.

Author Contribution Statement

Muhammad Ramli proposed the research problem, led the research, evaluated hydrogeological conditions, and drafted articles.

Aryanti Virtanti Anas proposed the research problem and was involved in conceptualization, dynamic systems modeling, and article drafting.

Asta Arjunoarwan Hatta conducted geological mapping, collected hydrological and climatological data, and created drawings.

Hasbi Bakri conducted geoelectric investigation and analysis and prepared drafts. All authors discussed the results and contributed to the final manuscript.

Conflict of interest

The authors declare no conflicts of interest regarding the publication of this manuscript.

References

[1] United Nations, *Groundwater Making the invisible visible*, *The United Nations World Water Development Report 2022*. [Online] Available: https://unesdoc.unesco.org/ark:/48223/pf0000380721

[2] Y.P. Cheng, F. Zhang, H. Dong, and X. Wen, "Groundwater and environmental challenges in Asia", *Journal of Groundwater Science and Engineering*, vol. 12, pp. 223−236, Jun. 2024. doi: https://doi.org/10.26599/JGSE.2024.9280017

[3] A. Guemouria, A. Chehbouni, S. Belaqziz, T,T, Epule, Y.A. Brahim, E.M.E.Khalki, D. Dhiba, and L. Bouchaou, "System dynamics approach for water resources management: A case study from the Souss-Massa Basin," *Water*, vol. 15, no. 8, 1506. Apr. 2023. doi: https://doi.org/10.3390/w15081506

[4] R. Taftazani, S. Kazama, and S. Takizawa, "Spatial analysis of groundwater abstraction and land subsidence for planning the piped water supply in Jakarta, Indonesia," *Water*, vol. 14, no. 20, 3197. Oct. 2022. doi: https://doi.org/10.3390/w14203197

[5] N. A. Radhi, A. S. T. Al-Madhhachi, and D. E. Sachit, "Groundwater Quality and Irrigation Suitability Assessment Using Geochemical and GIS-Based Approaches in Arid Regions," *Civil Engineering Journal*, vol. 11, no. 11, pp. 4536-4554, Nov. 2025. doi: http://dx.doi.org/10.28991/CEJ-2025-011-11-06

[6] M. Ramli and A. V. Anas, "Analysis of groundwater resources in the Majene coastal aquifer - Indonesia based on a hydrogeological conceptual model," *International Journal of Hydrology Science and Technology*, vol. 19, no. 3, pp. 309-328, Apr. 2025. doi: https://doi.org/10.1504/IJHST.2025.145547.

[7] R. W. Triweko, "The Threats to Urban Water Security of Indonesian Cities," In: M. Babel, A. Haarstrick, L. Ribbe, V. R. Shinde, N. Dichtl, (eds) *Water Security in Asia*, pp. 73-83, May 2021. doi: https://doi.org/10.1007/978-3-319-54612-4_6

[8] C. R. Priadi, E. Suleeman, L. Darmajanti, G. L. Putri, F. Genter, T. Foster, and J. Willetts, "Policy and regulatory context for self-supplied drinking water services in two cities in Indonesia: Priorities for managing risks," *Environmental Development*, vol. 49, 100940. Mar. 2024. doi: https://doi.org/10.1016/j.envdev.2023.100940

[9] Q. N. Pham, T. C. Nguyen, T. T. Ta, and T. L Tran, "Comprehensive approach to sustainable groundwater management in semi-arid Ninh Thuan plain, Vietnam," *Groundwater for Sustainable Development*, vol. 23, 101031, Nov. 2023. doi: https://doi.org/10.1016/j.gsd.2023.101031

[10] M. Khairulbahri. The qualitative analysis of the nexus dynamics in the Pekalongan coastal area, Indonesia. *Scientific Report,* vol. 12, 11391, July 2022. doi: https://doi.org/10.1038/s41598-022-15683-9

[11] L. R. Woolfenden, J. A. Engott, J. Larsen, and G. Cromwell, *Simulation of Groundwater and Surface-Water Resources of the San Antonio Creek Valley Watershed, Santa Barbara County, California*," U.S. Geological Survey Scientific Investigations Report 2021–5139, 76 p., Jan. 2022. doi: https://doi.org/10.3133/sir20215139

[12] J. A. Traum, N. F. Teague, D. S. Sweetkind, and T. Nishikawa, *Hydrologic and Geochemical Characterization of the Petaluma River watershed, Sonoma County, California*, U.S. Geological Survey Scientific Investigations Report 2022–5009, 217 p., Jan. 2022. doi: https://doi.org/10.3133/sir20225009

[13] G. Cromwell, D. S. Sweetkind, J. N. Densmore, J. A. Engott, W. A. Seymour, J. D. Larsen, C. P. Ely, C. L. Stamos, and C. C. Faunt, 2022, *Hydrogeologic Characterization of the San Antonio Creek Valley watershed, Santa Barbara County, California*, U.S. Geological Survey Scientific Investigations Report 2022–5001, 124 p., Jan. 2022. doi: https://doi.org/10.3133/sir20225001

[14] M. Ramli, Djamaluddin, M. Thamrin, and N. F. Qaidahiyani, "Hydrogeological conceptual model for estimating the groundwater storage in the Gowa-Takalar coastal aquifer, South Sulawesi", *Jurnal Teknik*, vol. 44, no. 1, pp. 85-96, Mei 2023, (in Bahasa Indonesia). doi: https://doi.org/10.14710/teknik.v44i1.34007

[15] Y. H. Huang, Y. J. Lai, and J. H. Wu, "A system dynamics approach to modeling groundwater dynamics: Case study of the Choshui River Basin," *Sustainability*, vol. 14, no. 1371, pp: 1-19. Jan. 2022. doi: https://doi.org/10.3390/su14031371

[16] M. S. Sardo and N. Jalalkamali, "A system dynamic approach for reservoir impact assessment on groundwater aquifer considering climate change scenario," *Groundwater for Sustainable Development.* vol. 17, May 2022. doi: https://doi.org/10.1016/j.gsd.2022.100754

[17] D. Secci, A. K. Saysel, İ. Uygur, O. C. Yoloğlu, A. Zanini, and N. K. Copty, "Modeling for sustainable groundwater management: Interdependence and potential complementarity of process-based, data-driven and system dynamics approaches," *Science of The Total Environment*, vol. 951, 175491, Nov. 2024. doi: https://doi.org/10.1016/j.scitotenv.2024.175491

[18] K. Naeem, S. Aloui, A. Zghibi, A. Mazzoni, C. Triki, and A. Elomri. "A system dynamics approach to management of water resources in Qatar," *Sustainable Production and Consumption,* vol. 46, pp. 733-753, May 2024. doi: https://doi.org/10.1016/j.spc.2024.03.024.

[19] M. A. Arasteh, and Y. Farjami, "New hydro-economic system dynamics and agent-based modeling for sustainable urban groundwater management: A case study of Dehno, Yazd Province, Iran," *Sustainable Cities and Society*, vol. 72, 103078, Sept. 2021. doi: https://doi.org/10.1016/j.scs.2021.103078

[20] Z. Yang, J. Song, D. Cheng, J. Xia, Q. Li, and M.I. Ahamad, "Comprehensive evaluation and scenario simulation for the water resources carrying capacity in Xi'an city, China," *J. Environ. Manag*. vol. 230, pp: 221–233, Jan. 2019. doi: https://doi.org/10.1016/j.jenvman.2018.09.085

[21] H. Abdolabadi, A. Sarang, M. Ardestani, and J. C. Little, "Estimating the available water in the watershed using system dynamics hydrological model. Case study: Ilam Watershed," *Environmental Energy and Economic Research*, vol. 2, no. 4: pp. 265–280, Jun. 2018. doi: https://doi.org/10.22097/eeer.2019.99210.1013.

[22] PAM Tirta Karajae *Groundwater Usage Report*, 2024, [Online] Available: https://pdamparepare.co.id (in Bahasa Indonesia).

[23] ESDM, *ESDM One Map: Exploring Energy and Mineral Resources of Indonesia, 2024* [Online]. Available: https://geoportal.esdm.go.id/home/metadata_html/97

[24] BPS-Statistic of Parepare Municipality, *Parepare Municipality in Figures 2020*, ISSN: 0215-7047. [Online] Available: https://pareparekota.bps.go.id/id/publication

[25] BPS-Statistic of Parepare Municipality, *Parepare Municipality in Figures 2021* ISSN: 0215-7047. [Online] Available: https://pareparekota.bps.go.id/id/publication

[26] BPS-Statistic of Parepare Municipality, *Parepare Municipality in Figures 2022* ISSN: 0215-7047. [Online] Available: https://pareparekota.bps.go.id/id/publication

[27] BPS-Statistic of Parepare Municipality, *Parepare Municipality in Figures 2023* ISSN: 0215-7047. [Online] Available: https://pareparekota.bps.go.id/id/publication

[28] BPS-Statistic of Parepare Municipality, *Parepare Municipality in Figures 2024* ISSN: 0215-704. [Online] Available: https://pareparekota.bps.go.id/id/publication

[29] R. Sukamto, *Geologic Map of The Pangkajene and Western Part of Watampone Quadrangles, Sulawesi*: Geological Research and Development Center, Bandung, 1982.

[30] P. Petrone, P. De Vita, P. Marsiglia, P. Allocca, S. Coda, D. Cusano, Lepore, and D Allocca, "Hydrogeological conceptual model and groundwater recharge of Avella Mts. Karst Aquifer (Southern Italy): A literature review and update," *Journal of Hydrology: Regional Studies*, vol. 54, no. 101871, pp: 1-19, Aug. 2024. doi: https://doi.org/10.1016/j.ejrh.2024.101871

[31] J. Doorenbos and W. O. Pruit, *Guidelines for Predicting Crop Water Requirements,* Food and Agriculture Organization of the United Nations, Rome, 1997.

[32] M. K. Goel, "Runoff Coefficient," In: Singh, V.P., Singh, P., Haritashya, U.K. (eds) *Encyclopedia of Snow, Ice and Glaciers. Encyclopedia of Earth Sciences Series*. Springer, Dordrecht. Jan. 2014. doi: https://doi.org/10.1007/978-90-481-2642-2_456

[33] A. Nurhakim, and M. Firdaus. "Opportunities for groundwater utilization to support the sustainability of water resources in Pare-Pare City," *Teknik Hidro*, vol. 15, no. 1, pp. 30–36, Feb. 2022. (in Bahasa Indonesia) [online] Available: https://journal.unismuh.ac.id/index.php/hidro/article/view/9799

[34] U. Sideng, S. Nyompa, and N.C. Rahayu. "Mapping of critically levels for cathment area (Case study of Parepare City)," *Jurnal Environmental Science*, vol. 4, no. 1, pp. 33-46, Oct. 2021 (in Bahasa Indonesia). doi: https://doi.org/10.35580/jes.v4i1.22393

[35] M. C. Peel, B. L. Finlayson, and T. A. McMahon, "Updated world map of the Koppen-Geiger climate classification," *Hydrology and Earth System Science*, vol. 11, pp. 1633–1644, Oct. 2007. doi: https://doi.org/10.5194/hess-11-1633-2007

[36] M. R. Kumar, S. R. Kumar, R. Thendiyath, and R. Jayakumar, "Assessment of water supply and demand in the lower mahi sub-basin using WEAP model", *The 10th International Conference on Future Environment and Energy*, Kyoto, Japan, Jan. 7-9, pp. 1-8, Dec. 2020. doi: https://doi.org/10.1088/1755-1315/581/1/012022

[37] *Preparation of spatial balance sheets of natural resources*; *Part 1 Water Resources*, SNI-6728.1:2015. (in Bahasa Indonesia)

[38] Minister of Public Works and Public Housing, *Regulation No. 27/PRT/M/2016 on the Implementation of Drinking Water Supply Systems,* 2016. [Online] Available: https://peraturan.bpk.go.id/Details/104463/permen-pupr-no-27-tahun-2016

Appendix-A: The SD Equation

Ground_Water_Balance(t) = Ground_Water_Balance(t - dt) + (Potential_for_New_Groundwater_Dev - Need_for_New__Groundwater_Dev) * dt

INIT Ground_Water_Balance = Potential_for_New_Groundwater_Dev- Need_for_New__Groundwater_Dev

INFLOWS:

Potential_for_New_Groundwater_Dev = Difference_between_Water_Balance_and_Groundwater_Production

OUTFLOWS:

Need_for_New__Groundwater_Dev = Lack_of_water_supply

Predicted_Population(t) = Predicted_Population(t - dt) + (Population) * dt

INIT Predicted_Population = 148265

INFLOWS:

Population = Predicted_Population*Growrate_population

Average_Monthly_Evapotranpiration = GRAPH(TIME)

(1.00, 119), (2.00, 104), (3.00, 122), (4.00, 129), (5.00, 138), (6.00, 115), (7.00, 134), (8.00, 187), (9.00, 187), (10.0, 189), (11.0, 152), (12.0, 128), (13.0, 119), (14.0, 104), (15.0, 122), (16.0, 129), (17.0, 138), (18.0, 115), (19.0, 134), (20.0, 187), (21.0, 187), (22.0, 189), (23.0, 152), (24.0, 128), (25.0, 119), (26.0, 104), (27.0, 122), (28.0, 129), (29.0, 138), (30.0, 115), (31.0, 134), (32.0, 187), (33.0, 187), (34.0, 189), (35.0, 152), (36.0, 128), (37.0, 119), (38.0, 104), (39.0, 122), (40.0, 129),

(41.0, 138), (42.0, 115), (43.0, 134), (44.0, 187), (45.0, 187), (46.0, 189), (47.0, 152), (48.0, 128), (49.0, 119), (50.0, 104), (51.0, 122), (52.0, 129), (53.0, 138), (54.0, 115), (55.0, 134), (56.0, 187), (57.0, 187), (58.0, 189), (59.0, 152), (60.0, 128), (61.0, 119), (62.0, 104), (63.0, 122), (64.0, 129), (65.0, 138), (66.0, 115), (67.0, 134), (68.0, 187), (69.0, 187), (70.0, 189), (71.0, 152), (72.0, 128), (73.0, 119), (74.0, 104), (75.0, 122), (76.0, 129), (77.0, 138), (78.0, 115), (79.0, 134), (80.0, 187), (81.0, 187), (82.0, 189), (83.0, 152), (84.0, 128), (85.0, 119), (86.0, 104), (87.0, 122), (88.0, 129), (89.0, 138), (90.0, 115), (91.0, 134), (92.0, 187), (93.0, 187), (94.0, 189), (95.0, 152), (96.0, 128), (97.0, 119), (98.0, 104), (99.0, 122), (100, 129), (101, 138), (102, 115), (103, 134), (104, 187), (105, 187), (106, 189), (107, 152), (108, 128), (109, 119), (110, 104), (111, 122), (112, 129), (113, 138), (114, 115), (115, 134), (116, 187), (117, 187), (118, 189), (119, 152), (120, 128)

Average_Monthly_Rainfall = GRAPH(TIME)

(1.00, 702), (2.00, 630), (3.00, 367), (4.00, 238), (5.00, 149), (6.00, 108), (7.00, 37.3), (8.00, 37.3), (9.00, 53.9), (10.0, 146), (11.0, 1349), (12.0, 661), (13.0, 702), (14.0, 630), (15.0, 367), (16.0, 238), (17.0, 149), (18.0, 108), (19.0, 37.3), (20.0, 37.3), (21.0, 53.9), (22.0, 146), (23.0, 1349), (24.0, 661), (25.0, 702), (26.0, 630), (27.0, 367), (28.0, 238), (29.0, 149), (30.0, 108), (31.0, 37.3), (32.0, 37.3), (33.0, 53.9), (34.0, 146), (35.0, 1349), (36.0, 661), (37.0, 702), (38.0, 630), (39.0, 367), (40.0, 238), (41.0, 149), (42.0, 108), (43.0, 37.3), (44.0, 37.3), (45.0, 53.9), (46.0, 146), (47.0, 1349), (48.0, 661), (49.0, 702), (50.0, 630), (51.0, 367), (52.0, 238), (53.0, 149), (54.0, 108), (55.0, 37.3), (56.0, 37.3), (57.0, 53.9), (58.0, 146), (59.0, 1349), (60.0, 661), (61.0, 702), (62.0, 630), (63.0, 367), (64.0, 238), (65.0, 149), (66.0, 108), (67.0, 37.3), (68.0, 37.3), (69.0, 53.9), (70.0, 146), (71.0, 1349), (72.0, 661), (73.0, 702), (74.0, 630), (75.0, 367), (76.0, 238), (77.0, 149), (78.0, 108), (79.0, 37.3), (80.0, 37.3), (81.0, 53.9), (82.0, 146), (83.0, 1349), (84.0, 661), (85.0, 702), (86.0, 630), (87.0, 367), (88.0, 238), (89.0, 149), (90.0, 108), (91.0, 37.3), (92.0, 37.3), (93.0, 53.9), (94.0, 146), (95.0, 1349), (96.0, 661), (97.0, 702), (98.0, 630), (99.0, 367), (100, 238), (101, 149), (102, 108), (103, 37.3), (104, 37.3), (105, 53.9), (106, 146), (107, 1349), (108, 661), (109, 702), (110, 630), (111, 367), (112, 238), (113, 149), (114, 108), (115, 37.3), (116, 37.3), (117, 53.9), (118, 146), (119, 1349), (120, 661)

Changes_in__Groundwater_Storage = (Average_Monthly_Rainfall-Average_Monthly_Evapotranpiration-Monthly_Surface_Runoff)

City_size = 89330

Coeficient_of_Runoff = 0.369

Cow__Buffalo_Horses = Predicted_Number__of_Livestock_1*Standard_Prediction_Farm_Water_Requirement

Difference_Between_Water_Balance_and_Groundwater_Production = Groundwater_Availability-(PAM_Groundwater__Production*RANDOM(0,9.1,1))

Domestic_Water_Demand = Domestic_Water__Demand_Standard*Predicted_Population

Domestic_Water__Demand_Standard = GRAPH(TIME)

(1.00, 3.41), (2.00, 3.08), (3.00, 3.41), (4.00, 3.30), (5.00, 3.41), (6.00, 3.30), (7.00, 3.41), (8.00, 3.41), (9.00, 3.30), (10.0, 3.41), (11.0, 3.30), (12.0, 3.41), (13.0, 3.41), (14.0, 3.08), (15.0, 3.41), (16.0, 3.30), (17.0, 3.41), (18.0, 3.30), (19.0, 3.41), (20.0, 3.41), (21.0, 3.30), (22.0, 3.41), (23.0, 3.30), (24.0, 3.41), (25.0, 3.41), (26.0, 3.08), (27.0, 3.41), (28.0, 3.30), (29.0, 3.41), (30.0, 3.30), (31.0, 3.41), (32.0, 3.41), (33.0, 3.30), (34.0, 3.41), (35.0, 3.30), (36.0, 3.41), (37.0, 3.41), (38.0, 3.08), (39.0, 3.41), (40.0, 3.30), (41.0, 3.41), (42.0, 3.30), (43.0, 3.41), (44.0, 3.41), (45.0, 3.30), (46.0, 3.41), (47.0, 3.30), (48.0, 3.41), (49.0, 3.41), (50.0, 3.08), (51.0, 3.41), (52.0, 3.30), (53.0, 3.41), (54.0, 3.30), (55.0, 3.41), (56.0, 3.41), (57.0, 3.30), (58.0, 3.41), (59.0, 3.30), (60.0, 3.41)

Goats = Standard_Prediction_Livestock_Water_Requirement_2*Predicted_Number__of_Livestock_2

Groundwater_Availability = Groundwater_Storage+(City_size*Changes_in__Groundwater_Storage)

Groundwater_Distribution = (Percentage_of__Groundwater_Loss*PAM_Groundwater__Production)

Groundwater_Storage = 528750

Growrate_population = 0.0011

Industrial_Water_Requirement_Standard = GRAPH(TIME)

(1.00, 37.2), (2.00, 33.6), (3.00, 37.2), (4.00, 36.0), (5.00, 37.2), (6.00, 36.0), (7.00, 37.2), (8.00, 37.2), (9.00, 36.0), (10.0, 37.2), (11.0, 36.0), (12.0, 37.2), (13.0, 37.2), (14.0, 33.6), (15.0, 37.2), (16.0, 36.0), (17.0, 37.2), (18.0, 36.0), (19.0, 37.2), (20.0, 37.2), (21.0, 36.0), (22.0, 37.2), (23.0, 36.0), (24.0, 37.2)

Industrial_Water__Requirements = Predicted_Number__of_Industries*Industrial_Water_Requirement_Standard

Lack_of_water_supply = Total_Water_Requirement-Groundwater_Distribution-PAM_Surface__Water_Production

Livestock_Water_Requirements = Goats+Cow__Buffalo_Horses+Poultry

Livestock_Water_Requirement_Standard_2 = GRAPH(TIME)

(1.00, 0.155), (2.00, 0.14), (3.00, 0.155), (4.00, 0.15), (5.00, 0.155), (6.00, 0.15), (7.00, 0.155), (8.00, 0.155), (9.00, 0.15), (10.0, 0.155), (11.0, 0.15), (12.0, 0.155), (13.0, 0.155), (14.0, 0.14), (15.0, 0.155), (16.0, 0.15), (17.0, 0.155), (18.0, 0.15), (19.0, 0.155), (20.0, 0.155), (21.0, 0.15), (22.0, 0.155), (23.0, 0.15), (24.0, 0.155), (25.0, 0.155), (26.0, 0.14), (27.0, 0.155), (28.0, 0.15), (29.0, 0.155), (30.0, 0.15), (31.0, 0.155), (32.0, 0.155), (33.0, 0.15), (34.0, 0.155), (35.0, 0.15), (36.0, 0.155), (37.0, 0.155), (38.0, 0.14), (39.0, 0.155), (40.0, 0.15), (41.0, 0.155), (42.0, 0.15), (43.0, 0.155), (44.0, 0.155), (45.0, 0.15), (46.0, 0.155), (47.0, 0.15), (48.0, 0.155), (49.0, 0.155), (50.0, 0.14), (51.0, 0.155), (52.0, 0.15), (53.0, 0.155), (54.0, 0.15), (55.0, 0.155), (56.0, 0.155), (57.0, 0.15), (58.0, 0.155), (59.0, 0.15), (60.0, 0.155)

Livestock_Water_Requirement_Standard_3 = GRAPH(TIME)

(1.00, 0.0186), (2.00, 0.0168), (3.00, 0.019), (4.00, 0.018), (5.00, 0.019), (6.00, 0.018), (7.00, 0.019), (8.00, 0.019), (9.00, 0.018), (10.0, 0.019), (11.0, 0.018), (12.0, 0.019), (13.0, 0.019), (14.0, 0.0168), (15.0, 0.019), (16.0, 0.018), (17.0, 0.019), (18.0, 0.018), (19.0, 0.019), (20.0, 0.019), (21.0, 0.018), (22.0, 0.019), (23.0, 0.018), (24.0, 0.019), (25.0, 0.019), (26.0, 0.017), (27.0, 0.019), (28.0, 0.018), (29.0, 0.019), (30.0, 0.018), (31.0, 0.019), (32.0, 0.019), (33.0, 0.018), (34.0, 0.019), (35.0, 0.018), (36.0, 0.019), (37.0, 0.019), (38.0, 0.017), (39.0, 0.019), (40.0, 0.018), (41.0, 0.019), (42.0, 0.018), (43.0, 0.019), (44.0, 0.019), (45.0, 0.018), (46.0, 0.019), (47.0, 0.018), (48.0, 0.019), (49.0, 0.019), (50.0, 0.017), (51.0, 0.019), (52.0, 0.018), (53.0, 0.019), (54.0, 0.018), (55.0, 0.019), (56.0, 0.019), (57.0, 0.018), (58.0, 0.019), (59.0, 0.018), (60.0, 0.019)

Monthly_Surface_Runoff = Coeficient_of_Runoff*Average_Monthly_Rainfall

Number_of_Industries = GRAPH(TIME)

(1.00, 1348), (2.00, 1348), (3.00, 1348), (4.00, 1348), (5.00, 1348), (6.00, 1348), (7.00, 1348), (8.00, 1348), (9.00, 1348), (10.0, 1348), (11.0, 1348), (12.0, 1348), (13.0, 1372), (14.0, 1372), (15.0, 1372), (16.0, 1372), (17.0, 1372), (18.0, 1372), (19.0, 1372), (20.0, 1372), (21.0, 1372), (22.0, 1372), (23.0, 1372), (24.0, 1372), (25.0, 1243), (26.0, 1243), (27.0, 1243), (28.0, 1243), (29.0, 1243), (30.0, 1243), (31.0, 1243), (32.0, 1243), (33.0, 1243), (34.0, 1243), (35.0, 1243), (36.0, 1243), (37.0, 1149), (38.0, 1149), (39.0, 1149), (40.0, 1149), (41.0, 1149), (42.0, 1149), (43.0, 1149), (44.0, 1149), (45.0, 1149), (46.0, 1149), (47.0, 1149), (48.0, 1149), (49.0, 1055), (50.0, 1055), (51.0, 1055), (52.0, 1055), (53.0, 1055), (54.0, 1055), (55.0, 1055), (56.0, 1055), (57.0, 1055), (58.0, 1055), (59.0, 1055), (60.0, 1055)

Number_of_Livestock_1 = GRAPH(TIME)

(1.00, 5457), (2.00, 5457), (3.00, 5457), (4.00, 5457), (5.00, 5457), (6.00, 5457), (7.00, 5457), (8.00, 5457), (9.00, 5457), (10.0, 5457), (11.0, 5457), (12.0, 5457), (13.0, 5077), (14.0, 5077), (15.0, 5077), (16.0, 5077), (17.0, 5077), (18.0, 5077), (19.0, 5077), (20.0, 5077), (21.0, 5077), (22.0, 5077), (23.0, 5077), (24.0, 5077), (25.0, 4812), (26.0, 4812), (27.0, 4812), (28.0, 4812), (29.0, 4812), (30.0, 4812), (31.0, 4812), (32.0, 4812), (33.0, 4812), (34.0, 4812), (35.0, 4812), (36.0, 4812), (37.0, 5431), (38.0, 5431), (39.0, 5431), (40.0, 5431), (41.0, 5431), (42.0, 5431), (43.0, 5431), (44.0, 5431), (45.0, 5431), (46.0, 5431), (47.0, 5431), (48.0, 5431), (49.0, 6050), (50.0, 6050), (51.0, 6050), (52.0, 6050), (53.0, 6050), (54.0, 6050), (55.0, 6050), (56.0, 6050), (57.0, 6050), (58.0, 6050), (59.0, 6050), (60.0, 6050)

Number_of_Livestock_2 = GRAPH(TIME)

(1.00, 3923), (2.00, 3923), (3.00, 3923), (4.00, 3923), (5.00, 3923), (6.00, 3923), (7.00, 3923), (8.00, 3923), (9.00, 3923), (10.0, 3923), (11.0, 3923), (12.0, 3923), (13.0, 3218), (14.0, 3218), (15.0, 3218), (16.0, 3218), (17.0, 3218), (18.0, 3218), (19.0, 3218), (20.0, 3218), (21.0, 3218), (22.0, 3218), (23.0, 3218), (24.0, 3218), (25.0, 2484), (26.0, 2484), (27.0, 2484), (28.0, 2484), (29.0, 2484), (30.0, 2484), (31.0, 2484), (32.0, 2484), (33.0, 2484), (34.0, 2484), (35.0, 2484), (36.0, 2484), (37.0, 2994), (38.0, 2994), (39.0, 2994), (40.0, 2994), (41.0, 2994), (42.0, 2994), (43.0, 2994), (44.0, 2994), (45.0, 2994), (46.0, 2994), (47.0, 2994), (48.0, 2994), (49.0, 3504), (50.0, 3504), (51.0, 3504), (52.0, 3504), (53.0, 3504), (54.0, 3504), (55.0, 3504), (56.0, 3504), (57.0, 3504), (58.0, 3504), (59.0, 3504), (60.0, 3504)

Number_of_Livestock_3 = GRAPH(TIME)

(1.00, 1.3e+006), (2.00, 1.3e+006), (3.00, 1.3e+006), (4.00, 1.3e+006), (5.00, 1.3e+006), (6.00, 1.3e+006), (7.00, 1.3e+006), (8.00, 1.3e+006), (9.00, 1.3e+006), (10.0, 1.3e+006), (11.0, 1.3e+006), (12.0, 1.3e+006), (13.0, 977794), (14.0, 977794), (15.0, 977794), (16.0, 977794), (17.0, 977794), (18.0, 977794), (19.0, 977794), (20.0, 977794), (21.0, 977794), (22.0, 977794), (23.0, 977794), (24.0, 977794), (25.0, 818344), (26.0, 818344), (27.0, 818344), (28.0, 818344), (29.0, 818344), (30.0, 818344), (31.0, 818344), (32.0, 818344), (33.0, 818344), (34.0, 818344), (35.0, 818344), (36.0, 818344), (37.0, 811027), (38.0, 811027), (39.0, 811027), (40.0, 811027), (41.0, 811027), (42.0, 811027), (43.0, 811027), (44.0, 811027), (45.0, 811027), (46.0, 811027), (47.0, 811027), (48.0, 811027), (49.0, 804904), (50.0, 804904), (51.0, 804904), (52.0, 804904), (53.0, 804904), (54.0, 804904), (55.0, 804904), (56.0, 804904), (57.0, 804904), (58.0, 804904), (59.0, 804904), (60.0, 804904)

Number_of_Wells = 13

PAM_Groundwater__Production = Number_of_Wells*Wells_capacity

PAM_Surface__Water_Production = 233329

Percentage_of__Groundwater_Loss = 0.4722

Poultry = Predicted_Number__of_Livestock_3*Standard_Prediction_Livestock_Water_Requirement_3

Predicted_Number__of_Industries = RANDOM(1000,1500,Number_of_Industries)

Predicted_Number__of_Livestock_1 = RANDOM(4800,6100, Number_of_Livestock_1)

Predicted_Number__of_Livestock_2 = RANDOM(2000,4500,Number_of_Livestock_2)

Predicted_Number__of_Livestock_3 = RANDOM(800000,1000000,Number_of_Livestock_3)

Requirement_Standard_Farm_Water = GRAPH(TIME)

(1.00, 1.24), (2.00, 1.12), (3.00, 1.24), (4.00, 1.20), (5.00, 1.24), (6.00, 1.20), (7.00, 1.24), (8.00, 1.24), (9.00, 1.20), (10.0, 1.24), (11.0, 1.20), (12.0, 1.24), (13.0, 1.24), (14.0, 1.12), (15.0, 1.24), (16.0, 1.20), (17.0, 1.24), (18.0, 1.20), (19.0, 1.24), (20.0, 1.24), (21.0, 1.20), (22.0, 1.24), (23.0, 1.20), (24.0, 1.24), (25.0, 1.24), (26.0, 1.12), (27.0, 1.24), (28.0, 1.20), (29.0, 1.24), (30.0, 1.20), (31.0, 1.24), (32.0, 1.24), (33.0, 1.20), (34.0, 1.24), (35.0, 1.20), (36.0, 1.24), (37.0, 1.24), (38.0, 1.12), (39.0, 1.24), (40.0, 1.20), (41.0, 1.24), (42.0, 1.20), (43.0, 1.24), (44.0, 1.24), (45.0, 1.20), (46.0, 1.24), (47.0, 1.20), (48.0, 1.24), (49.0, 1.24), (50.0, 1.12), (51.0, 1.24), (52.0, 1.20), (53.0, 1.24), (54.0, 1.20), (55.0, 1.24), (56.0, 1.24), (57.0, 1.20), (58.0, 1.24), (59.0, 1.20), (60.0, 1.24)

Standard_Prediction_Farm_Water_Requirement = RANDOM(1.2,1.24,Requirement_Standard_Farm_Water)

Standard_Prediction_Livestock_Water_Requirement_2 = RANDOM(0.14,0.155,Livestock_Water_Requirement_Standard_2)

Standard_Prediction_Livestock_Water_Requirement_3 = RANDOM(0.017,0.019,Livestock_Water_Requirement_Standard_3)

Total_Water_Requirement = Domestic_Water_Demand+Industrial_Water__Requirements+ Livestock_Water_Requirements

Wells_capacity = 29,018.36